

Topological protection of photonic path entanglement

MIKAEL C. RECHTSMAN,^{1,*} YAAKOV LUMER,² YONATAN PLOTNIK,² ARMANDO PEREZ-LEIJA,³
ALEXANDER SZAMEIT,³ AND MORDECHAI SEGEV²

¹Department of Physics, The Pennsylvania State University, University Park, Pennsylvania 16802, USA

²Department of Physics, Technion—Israel Institute of Technology, Haifa 32000, Israel

³Institute of Applied Physics, Friedrich-Schiller-Universität, Jena, Germany

*Corresponding author: mcrworld@psu.edu

Received 3 May 2016; revised 28 June 2016; accepted 30 June 2016 (Doc. ID 263381); published 23 August 2016

The recent advent of photonic topological insulators has opened the door to using the robustness of topologically protected transport—originated in the domain of condensed matter physics—in optical devices and in quantum simulation. Concurrently, quantum walks in photonic networks have been shown to yield exponential speedup for certain algorithms, such as Boson sampling. Here we theoretically demonstrate that photonic topological insulators can robustly protect the transport of quantum information through photonic networks, despite the presence of disorder. © 2016

Optical Society of America

OCIS codes: (270.0270) Quantum optics; (000.1600) Classical and quantum physics; (050.5298) Photonic crystals.

<http://dx.doi.org/10.1364/OPTICA.3.000925>

Topological insulators are materials that have a bulk bandgap, but have edge (or surface) states with energies that cross the gap [1]. In 2D, these states are protected from scattering: they cannot scatter into the bulk due to the gap, and they cannot scatter backward because the backward channel is not present or is forbidden from coupling. This leads to robust transport, offering potential applications in quantum information [1], wherein qubits are protected against decoherence.

Photonic topological insulators (PTIs) were proposed [2,3] and realized in microwaves [4,5]. Other schemes were then predicted for the optical regime [6–9] and realized in experiments using arrays of helical waveguides [10] and in resonator arrays [11]. As described below, here we are interested in the system of Ref. [10], where classical light in the paraxial regime (thus obeying a Schrödinger-type paraxial wave equation) propagates in a honeycomb lattice of helical waveguides. In such a helical honeycomb lattice, a bandgap exists in the spatial spectrum with topological edge states. Each of the bands acquires a nonzero Chern number. The experiment showed that even in the presence of scattering (by defects and corners), the edge wave function propagates unimpeded.

Independently, quantum walks [12] in photonic lattices have shown rich physics [13–16]. A breakthrough came in 2013, when it was shown that non-interacting quantum walks give exponential speedups in calculating hard-to-compute quantities [17]; this is “boson sampling”. This, taken together with the “KLM protocol,” [18] shows that non-interacting optical systems show great potential for quantum information processing. As of yet, however, there has been no notion on how topological photonic systems can “topologically protect” quantum information. Indeed, there

is no need to protect photons from decoherence because photons barely interact and decohere slowly. So what does it mean to protect photonic quantum information?

Here, we show that PTIs can be used to robustly transport fragile multiphoton states in quantum walks. We show that these states maintain their path entanglement despite disorder, in stark contrast with nontopological systems. Throughout this analysis the topological nature of the system is manifested in the robust transport of its unidirectional propagating edge states, where scattering by defects and imperfections is suppressed.

First, we show using a simplified analytical argument that scattering will necessarily destroy maximally spatially entangled states (for example, two-particle NOON states [19,20], where the measurement of a photon in one channel implies that the other will be observed in the same one). Specifically, we show that upon backscattering any initially NOON-state wave packet will necessarily contain a nonzero amplitude to measure one transmitted and one reflected photon, making the wave function non-NOON. We then use numerical simulations to show that path entanglement is preserved in a disordered topological system, and destroyed in a topologically trivial system.

Consider the diagram of the 1D nontopological lattice with a defect (Fig. 1). The two single-photon spatial states in which the photons are initially launched are $I_l^\dagger|0\rangle$ and $I_r^\dagger|0\rangle$ (denoting left and right wave packets, where I_l^\dagger creates a photon in the left state and I_r^\dagger in the right state). We allow the wave packets to hit the defect and be reflected and transmitted. Assuming that both the left and right wave packets get reflected and transmitted with the amplitudes r and t , we have

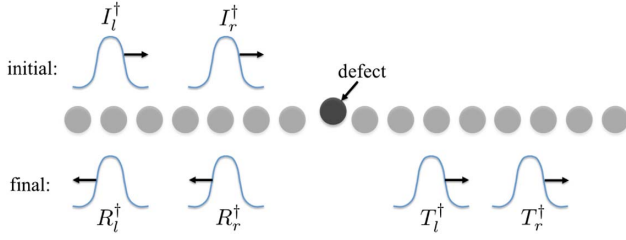


Fig. 1. We consider an injected NOON state based on spatially separated input states. They scatter off a defect in the topologically trivial 1D lattice, resulting in reflected and transmitted wave packets.

$$\begin{aligned} I_l^\dagger &\rightarrow \mathcal{U}I_l^\dagger\mathcal{U}^\dagger = rR_l^\dagger + tT_l^\dagger \quad \text{and} \\ I_r^\dagger &\rightarrow \mathcal{U}I_r^\dagger\mathcal{U}^\dagger = rR_r^\dagger + tT_r^\dagger, \end{aligned} \quad (1)$$

where \mathcal{U} denotes the evolution operator corresponding to the field Hamiltonian (not the single-particle evolution operator in the Schrödinger picture); and R_l^\dagger (T_l^\dagger) and R_r^\dagger (T_r^\dagger) are the left and right reflected (transmitted) wave packets, respectively. Consider an initial NOON state: $|\psi(0)\rangle = \frac{1}{2}(I_l^\dagger I_l^\dagger + I_r^\dagger I_r^\dagger)|0\rangle$.

After the state evolves and gets reflected from and transmitted by the defect, the wave function is:

$$\begin{aligned} |\psi(0)\rangle &\rightarrow |\psi(t)\rangle = \frac{1}{2}\mathcal{U}(I_l^\dagger I_l^\dagger + I_r^\dagger I_r^\dagger)\mathcal{U}^\dagger|0\rangle \\ &= \frac{1}{2}[(\mathcal{U}I_l^\dagger\mathcal{U}^\dagger)(\mathcal{U}I_l^\dagger\mathcal{U}^\dagger) + (\mathcal{U}I_r^\dagger\mathcal{U}^\dagger)(\mathcal{U}I_r^\dagger\mathcal{U}^\dagger)]|0\rangle. \\ &= \frac{1}{2}[(rR_l^\dagger + tT_l^\dagger)(rR_l^\dagger + tT_l^\dagger) + (rR_r^\dagger + tT_r^\dagger)(rR_r^\dagger + tT_r^\dagger)]|0\rangle \\ &= \frac{1}{2}[r^2R_l^\dagger R_l^\dagger + t^2T_l^\dagger T_l^\dagger + 2trT_l^\dagger R_l^\dagger + r^2R_r^\dagger R_r^\dagger \\ &\quad + t^2T_r^\dagger T_r^\dagger + 2trT_r^\dagger R_r^\dagger]|0\rangle. \end{aligned} \quad (2)$$

This state is fundamentally non-NOON, because of the amplitudes that mix the transmitted state on the right and the reflected state on the left (and vice versa)—these are the cross terms. Note that if one considers only the region on the right-hand side of the defect, the state is NOON-like. However, in this toy model the reflected channel must not be ignored, since wave packets therein may (in a more complex setting) encounter another defect and get scattered in the rightward direction. This would therefore make the overall transmitted state most definitely non-NOON. Indeed, in a fully disordered system, the state will be less NOON-like with each scattering event, hence, the final state is necessarily some random state that is not maximally path entangled. This simplified model also conveys why the path-entanglement character is not destroyed in topologically protected lattices. If $r = 0$ (a property of topological protection), clearly there are no cross terms and the state remains NOON.

To study a quantum walk in a PTI lattice, consider a honeycomb lattice of helical waveguides akin to the design in Ref. [10], and as depicted in Fig. 2(a), i.e., a PTI. The dynamics of the diffraction of a photon through a PFTI waveguide array is given by [10]

$$i\partial_z a_n^\dagger = \sum_{\langle m \rangle} c e^{iA_0(\cos \Omega z, \sin \Omega z) \cdot \mathbf{r}_{nm}} a_m^\dagger + u_n a_n^\dagger \equiv \sum_m H_{nm}(z) a_m^\dagger, \quad (3)$$

where z is the distance of propagation along the waveguide axis; a_n^\dagger creates a photon on waveguide n ; c is the coupling; $A_0 = kR\Omega a$ is

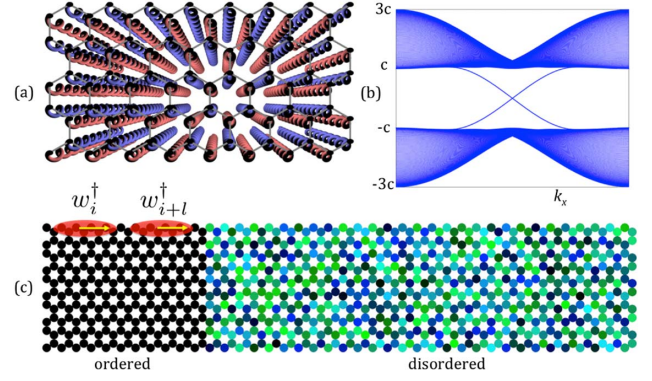


Fig. 2. (a) Honeycomb lattice of helical waveguides forms a PFTI [10]. (b) The band structure in the topological case (edge states cross the bandgap). (c) The probing effects of disorder: the two-photon state is injected in the “clean” region (left), and enters the disordered region (right).

the gauge field strength (arising due to the helicity); k is the wavenumber, R is the helix radius, Ω is the spatial frequency of the helices and a is the lattice constant; u_n is a random number lying in the range $[-W, W]$, representing disorder (random waveguide refractive index); and $H^F(z)$ is the z -dependent Schrödinger-picture Hamiltonian. Here, z takes the place of time in the usual Schrödinger equation. Physical time can be fully neglected in the case of continuous-wave light. Or, if pulsed lasers are used, chromatic dispersion effects can be neglected when the hopping constant c does not change significantly within the spectral bandwidth of 10 nm or less, corresponding to pulses of several hundred femtoseconds, is more than sufficient. Since z , the propagation distance, acts like time, the photon diffraction maps to the temporal motion of a quantum particle. This mathematical equivalence between Eq. (3) and the Schrödinger equation has been exploited to probe a wealth of phenomena, including Bloch oscillations [21,22], Zener tunneling [23], Shockley states [24], bound states in the continuum [25], Anderson localization [26–28], photonic quasicrystals [29], photonic graphene [30], and others.

It has been shown [31] that Floquet topological insulators in the strong-driving limit (helix pitch smaller than coupling length), the z dependence can be removed and the system can be approximately described by the Haldane model [32]. We work exclusively in this limit. The practical difference between the two lies in the fact that there is some bending loss associated with the waveguide helicity. Experimentally, this will manifest in a lower photon count, meaning that a longer integration time is required. But this does not affect photon correlations in the lattice.

This photonic system exhibits topological edge states residing in the bulk gap [10,32], as shown in see Fig. 2(b). Moreover, there are no counterpropagating states in the gap, meaning that when the edge states encounter a defect they do not scatter. In the Haldane model, we consider a honeycomb lattice with nearest neighbor coupling term c_1 , the second-neighbor term $|c_2| = 0.2|c_1|$; the coupling phase is set to $\pi/2$ [32]. This regime is easily accessed in the model in Ref. [10]. The bandgap is called topological because there is a nonzero topological invariant (the Chern number—see Ref. [32]). The edge states travel to the right along the upper edge and to the left along the bottom edge.

To elucidate the role of the topological features of our system in protecting entanglement, consider the specific system sketched in Fig. 2(c). This is essentially the photonic topological insulator of Ref. [10], with the left part of it being an ideal (disorder-free) lattice, whereas the right part of it contains disorder. States are injected on the “clean” left side (i.e., not disordered; $W = 0$), propagate to the right, and enter a disordered region. The goal here is to examine the effect of the disordered region on the properties of a two-photon wave function. We note in addition that here we restrict our analysis to pure quantum states being launched into the waveguide array rather than mixed states. That said, the correlation map associated with ideal NOON states cannot arise from classical light of any form (see the criteria for classical light set forth in Ref. [14], which NOON states violate).

Photonic quantum walks involve injecting a photon into a waveguide, or multiple photons in path-entangled spatial states [13–16]. Our initial state is a superposition of topological edge states. In particular, consider the projection of a single waveguide excitation on only edge modes in the bandgap (which can be achieved experimentally through the use of a spatial light modulator to launch the exact wave function). We construct these states from the edge states in the bandgap within some finite spatial bandwidth, centered in the middle of the gap such that $|E| < E_b$ (where E represents the energy of the state, and $2E_b$ is the spatial bandwidth). We note here that at the center of the bandgap [see Fig. 2(b)], the topological edge state is at an inflection point. At that point, the second-order diffraction term is zero. Therefore, the amount of diffraction of the wave packet will approach zero more quickly with increasing wave packet size than at any other point in the band structure. Therefore, choosing this point to be spectrally at the center (as we have done here) allows for the smallest possible wave packets for a given tolerance for diffraction. A large spatial bandwidth means that the edge wave function has a small spatial extent, whereas a small one means a larger extent along the edge. We call w_n^\dagger the operator that creates a photon in the state centered on waveguide n . These wave functions, which are localized to the top edge of the lattice, are depicted by the red ellipses in Fig. 2(c). They propagate to the right and enter the disordered region [depicted in Fig. 2(c)]. Since the edge states only occupy a fraction of the complete spectrum, the wave packets are “sinc-like”, i.e., they have decaying outer lobes. Despite the disorder, since the waveguide array acts as a completely closed system obeying deterministic dynamics, there is no mechanism that can lead to a loss of phase coherence (i.e., there is no external bath). Thus, a multiphoton wave function entering the array in a pure state remains in one.

Now, consider the injection of two path-entangled photons along the edge. The initial wave function, which contains the amplitude to observe a photon at waveguides m and n can be written $|\psi(z=0)\rangle = \sum_{mn} \epsilon_{mn} a_m^\dagger a_n^\dagger |0\rangle$. The correlation map is given by $\Gamma_{mn}(z) = \langle \psi(z) | a_m^\dagger a_n^\dagger a_n a_m | \psi(z) \rangle$ [16] for the two-photon wave function $|\psi(z)\rangle$ at propagation distance z . As we show in Supplement 1, Γ_{mn} at any propagation distance z can be written in terms of the one-photon propagator $U(z) = e^{-iHz}$, as $\Gamma_{mn} = |(U(c + c^T)U^T)_{mn}|^2$. Although this expression is general, henceforth we use m and n to index waveguides along only the edge, not the bulk. The expression $P_{mn} = \Gamma_{mn}/(1 + \delta_{mn})$ gives the probability of observing one photon in waveguide m and another photon in n .

We study the dynamics of two distinct two-photon initial states: a NOON state [19,20], namely, $|\psi_{\text{NOON}}\rangle = (w_i^\dagger w_i^\dagger +$

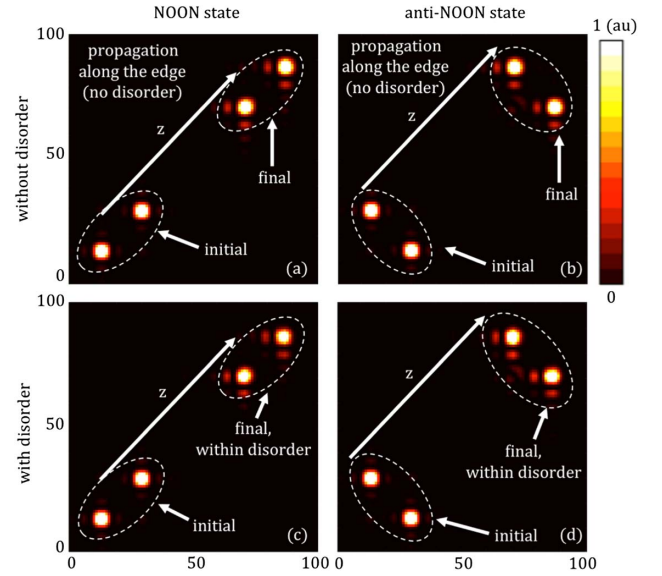


Fig. 3. Correlation map evolution along the edge of the photonic topological insulator depicted in Fig. 2(c) for: (a) the NOON state with no disorder; (b) the anti-NOON state with no disorder; (c) the NOON state with disorder; (d) the anti-NOON state with disorder. The disorder starts half way through. Here we see that the presence of disorder has not caused a strong change in the qualitative behavior of the correlation map (see Fig. 4 for a comparison with the topologically trivial case).

$w_{i+l}^\dagger w_{i+l}^\dagger |0\rangle/2$ as well as an “anti-NOON” but still indistinguishable photon state $|\psi_{\text{SEP}}\rangle = (w_i^\dagger w_{i+l}^\dagger |0\rangle$. Here, l indexes the number of waveguides between the states; we take $l = 16$. These states may be constructed experimentally using parametric down-conversion and beam shaping with a spatial light modulator.

Figure 3 shows the dynamics of the two-photon states in two cases: for a nondisordered topological system (first row), and for a similar system but with the right section highly disordered (second row), corresponding to Fig. 2(c). For all cases, the disorder strength is $W = c/2$. We choose this value of the disorder because it is large enough to cause significant scattering in the trivial case, but not large enough to close the topological gap, negating the topological protection. The first column is for two-photon NOON states, and the second is for anti-NOON states. The disordered region contains random on-site energies (i.e., the refractive indices) within the range $[-W, W]$. Each subfigure here shows the correlation map Γ_{mn} , just for the edge waveguides. The initial state (shown at the bottom-left corner of each subfigure) is composed of two lobes denoting the position of the injection of photons. For the NOON states, these lobes lie along the diagonal (meaning that if one photon is observed centered on waveguide n , the other must be centered there as well). For the anti-NOON state, the opposite is true: if one photon is centered at n , the other must be centered on $n + l$, meaning that the lobes lie across the diagonal from one another.

In Figs. 3(a) and 3(b), which correspond to the nondisordered case, the NOON and anti-NOON states travel along the diagonal (corresponding to moving rightward along the edge) and undergo some degree of diffractive broadening. The broadening is weak because the topological edge state, since it crosses the band gap, has a nearly linear dispersion [see Fig. 2(b)]. Of course the wavefunction eventually diffractively broadens due to higher-order diffraction

terms. The diffractive broadening can be reduced by decreasing the spatial bandwidth of the input wave function $2E_b$ (resulting in a wider wave function). It can therefore be suppressed to any desired degree.

Figures 3(c) and 3(d) represent the case where the photons enter a disordered region [but are otherwise analogous to 3(a) and 3(b)]. Note that for both the NOON and anti-NOON cases, the path-entangled photons pass through mostly unchanged, despite the disorder. For the NOON state, the “NOONity” (precisely defined below) of the state is preserved. This is striking considering that photon correlations are highly sensitive to the phase of the one-particle propagator; therefore, not only does topological protection preserve the one-particle state in the disordered region, but also the nature of the path entanglement of two-particle states. This happens despite the fact that the defects imbue the state with a random phase compared to the clean case. Animations of the dynamics associated with the correlation map shown in Fig. 3 are given in Visualization 1, Visualization 2, Visualization 3, and Visualization 4.

We also compare the protection of the two-particle state in the topological case to what occurs in the nontopological case. Perhaps the best way of doing this is to simply remove the bulk and study the edge in isolation; without the bulk to provide a buffer between the top and bottom edges of the lattice, the system ceases to be topological and backscattering is permitted. Therefore, we consider a 1D lattice with a coupling term of strength c between sites (akin to Fig. 1). We launch two entangled photons into the 1D lattice, analogously to the top edge of the 2D topological case. Figure 4 shows the correlation map for the NOON state wave function (top row is the clean case, bottom row is the disordered). The left column represents the initial state, and the next columns represent the wave function after successively longer propagation distances. Clearly, the clean and disordered cases behave entirely differently; as a result of backscattering, the NOONity of the photons is destroyed in the nontopological lattice. A similar picture emerges for the anti-NOON state.

To quantify this, we introduce a quantity that measures the nature of path entanglement: the “NOONity” N of a two-photon state

$$N \equiv \sum_{mn} \Gamma_{mm} \Gamma_{nn} - \Gamma_{mn}^2$$

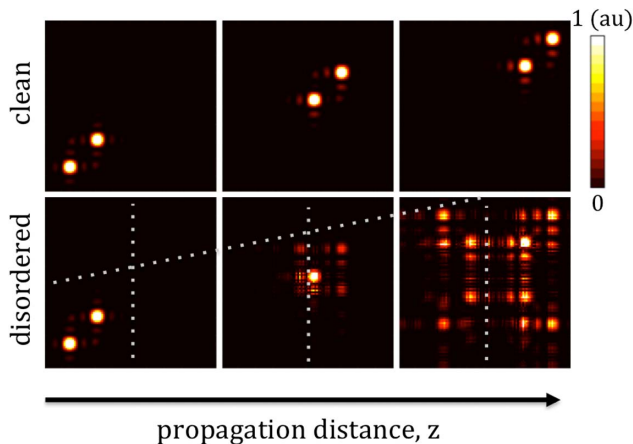


Fig. 4. Figures show the correlation map evolution in the topologically trivial 1D array for NOON states, in two cases: without (top row) and with (bottom row) disorder present. It is clear that the defect destroys the nature of the photon correlations (disorder interface at dotted line).

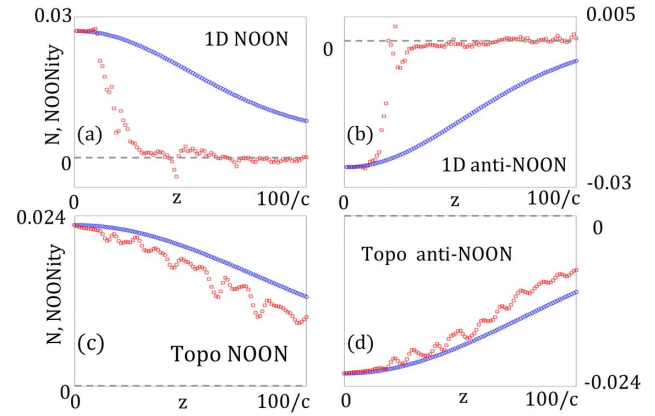


Fig. 5. Evolution of the “NOONity” as a function of z for: (a) a NOON state on the nontopological edge; (b) an anti-NOON state on the nontopological edge; (c) a NOON state on the topological edge; (d) an anti-NOON state on the topological edge. In the topologically trivial cases (a) and (b), NOONity and anti-NOONity are destroyed by disorder, whereas in the topological cases (c) and (d) they are largely conserved. The blue points indicate the clean case (disorder, $W = 0$); the red points indicate the disordered case ($W = c/2$).

The larger this quantity, the more NOON-like is the state. It is positive for a NOON state, zero for a nonspatially entangled state (e.g., a state that represents two photons in the same single-photon state) and negative for an anti-NOON state. In Fig. 5, we plot N as a function of z , in order to compare the shape of the wave function with and without disorder. In Fig. 5(a) the NOON state is in the topologically trivial 1D array; 5(b) the anti-NOON state in the same; 5(c) the NOON state on the topological edge; and 5(d) the anti-NOON state in the same. In all cases in Fig. 5 (including the nondisordered case), there is some decrease in N caused by unavoidable diffractive broadening (choosing a wave packet covering ~ 10 waveguides leads to a decrease in NOONity of $\sim 1/2$ over 100 coupling lengths).

Now comparing to the disordered case, in both Figs. 5(a) and 5(b), we see that the disorder has destroyed the NOON and anti-NOON states in the nontopological system. By comparison, in Figs. 5(c) and 5(d), which show the topological case, we see that the character of the state is largely preserved. This is depicted in Fig. 3 as well as in the visualizations. (See Visualization 1, Visualization 2, Visualization 3, Visualization 4, Visualization 5, Visualization 6, Visualization 7, and Visualization 8.) Clearly, the topological protection has protected the character of the state, preserving the “NOONity” of both the NOON and anti-NOON states. We account for the deviation between the clean and disordered topological cases as follows. When topological edge states propagate past a defect unscattered they effectively “go around it,” meaning it takes them an additional amount of time (z) compared with a clean system. We therefore interpret the difference between the clean and disordered case shown in Figs. 5(c) and 5(d) as the edge states taking “longer” to traverse the disordered path. As a result of diffractive broadening, there is some decrease in NOONity in the disordered case compared with the clean one (though much less than in the nontopological case). This can be seen by comparing Figs. 3(a) and 3(c); careful examination shows that the final state in each case is not exactly the same, with minor qualitative differences. For example, the higher-order diffractive lobes are more pronounced in the latter

(disordered) case compared to the former (clean) case. This is consistent with the state effectively propagating a longer distance due to the disorder, since diffractive lobes of course become more pronounced with distance from the source. The same can be said of Figs. 3(b) and 3(d).

Before closing, it is important to discuss experimental realizations and potential obstacles. The proposed system is the same as in [10], and the NOON edge states will be launched by use of two spatial light modulators to properly engineer the spatial wave functions of NOON states generated, as in [20]. We expect the principle challenges associated with an experiment to be threefold: (1) shaping the spatial wave function to sufficiently overlap the topological edge states such that bulk states do not interfere with the dynamics; (2) fully optimizing experimental parameters to minimize absorption, scattering, and bending losses associated with the waveguides in order to achieve high photon counts; and (3) collecting the photons from all of the waveguides at the output facet with a high coupling efficiency. For (1), a sufficiently high-resolution phase-modulated spatial light modulator should give enough control over the wave function to realize a high edge state overlap; for (2) this will depend on the specifics of the waveguides but previous work showing less than 1 dB/cm total loss well into the topological phase [10] is reasonable and can likely be improved upon; and (3) specially designed integrated fiber couplers can be used to directly couple to pigtailed waveguides. Taken together, we believe the experiment can be realistically carried out.

In conclusion, we have shown that topological edge states can transport path-entangled multiphoton states in a robust way, demonstrating that photonic topological insulators have clear advantages in transporting quantum light. In this work, we have only dealt with pure quantum states, not mixed states. However, we expect our results to straightforwardly generalize to that case as well, but a full analysis will require integrating the density of the matrix of the system, rather than simply the deterministic evolution of biphoton states. We further note that, since the argument captured in Eq. (2) generalizes to a higher photon number, the protection of NOONity described here should similarly generalize to that case as well. The effect presented here may lead to robust transport of quantum information through disordered environments, and provokes many new questions. For example, what happens to the topological protection in the presence of photon interactions? To what extent is photonic topological protection compatible with networks that are useful for quantum information applications?

Note: This work was presented in the 2015 conference on lasers and electro-optics (CLEO) [33]. After the submission of this manuscript we became aware of another work proposing a similar effect in the temporal domain [34].

Funding. National Science Foundation (NSF) (ECCS-1509546); Alfred P. Sloan Foundation (FG-2016-6418); Deutsche Forschungsgemeinschaft (DFG) (SZ 276/9-1, SZ 276/7-1, BL 574/13-1); European Commission (EC) (691209); Israeli Centers for Research Excellence (I-CORE).

Acknowledgment. M.S acknowledges support from the European Commission under project NHQWAVE, number 691209, and the Israeli Excellence Center ICORE on ‘Light and Matter’.

See Supplement 1 for supporting content.

REFERENCES

1. M. Z. Hasan and C. L. Kane, “Colloquium: Topological insulators,” *Rev. Mod. Phys.* **82**, 3045–3067 (2010).
2. F. D. M. Haldane and S. Raghu, “Possible realization of directional optical waveguides in photonic crystals with broken time-reversal symmetry,” *Phys. Rev. Lett.* **100**, 013904 (2008).
3. Z. Wang, Y. D. Chong, J. D. Joannopoulos, and M. Soljačić, “Reflection-free one-way edge modes in a gyromagnetic photonic crystal,” *Phys. Rev. Lett.* **100**, 013905 (2008).
4. Z. Wang, Y. Chong, J. D. Joannopoulos, and M. Soljačić, “Observation of unidirectional backscattering-immune topological electromagnetic states,” *Nature* **461**, 772–775 (2009).
5. X. Cheng, C. Jouvau, X. Ni, S. H. Mousavi, A. Z. Genack, and A. B. Khanikaev, “Robust reconfigurable electromagnetic pathways within a photonic topological insulator,” *Nat. Mater.* **15**, 542–548 (2016).
6. R. O. Umucallilar and I. Carusotto, “Artificial gauge field for photons in coupled cavity arrays,” *Phys. Rev. A* **84**, 043804 (2011).
7. M. Hafezi, E. A. Demler, M. D. Lukin, and J. M. Taylor, “Robust optical delay lines with topological protection,” *Nat. Phys.* **7**, 907–912 (2011).
8. K. Fang, Z. Yu, and S. Fan, “Realizing effective magnetic field for photons by controlling the phase of dynamic modulation,” *Nat. Photonics* **6**, 782–787 (2012).
9. A. B. Khanikaev, S. Hossein Mousavi, W.-K. Tse, M. Kargarian, A. H. MacDonald, and G. Shvets, “Photonic topological insulators,” *Nat. Mater.* **12**, 233–239 (2013).
10. M. C. Rechtsman, J. M. Zeuner, Y. Plotnik, Y. Lumer, D. Podolsky, F. Dreisow, S. Nolte, M. Segev, and A. Szameit, “Photonic Floquet topological insulators,” *Nature* **496**, 196–200 (2013).
11. M. Hafezi, S. Mittal, J. Fan, A. Migdall, and J. M. Taylor, “Imaging topological edge states in silicon photonics,” *Nat. Photonics* **7**, 1001–1005 (2013).
12. Y. Aharonov, L. Davidovich, and N. Zagury, “Quantum random walks,” *Phys. Rev. A* **48**, 1687–1690 (1993).
13. H. B. Perets, Y. Lahini, F. Pozzi, M. Sorel, R. Morandotti, and Y. Silberberg, “Realization of quantum walks with negligible decoherence in waveguide lattices,” *Phys. Rev. Lett.* **100**, 170506 (2008).
14. Y. Bromberg, Y. Lahini, R. Morandotti, and Y. Silberberg, “Quantum and classical correlations in waveguide lattices,” *Phys. Rev. Lett.* **102**, 253904 (2009).
15. Y. Lahini, Y. Bromberg, D. N. Christodoulides, and Y. Silberberg, “Quantum correlations in two-particle Anderson localization,” *Phys. Rev. Lett.* **105**, 163905 (2010).
16. A. Peruzzo, M. Lobino, J. C. F. Matthews, N. Matsuda, A. Politi, K. Poulios, X.-Q. Zhou, Y. Lahini, N. Ismail, K. Wörhoff, Y. Bromberg, Y. Silberberg, M. G. Thompson, and J. L. O’Brien, “Quantum walks of correlated photons,” *Science* **329**, 1500–1503 (2010).
17. S. Aaronson and A. Arkhipov, “The computational complexity of linear optics,” in *Proceedings of the 43rd Annual ACM Symposium on Theory of Computing (ACM, 2011)*, pp. 333–342.
18. E. Knill, R. Laflamme, and G. J. Milburn, “A scheme for efficient quantum computation with linear optics,” *Nature* **409**, 46–52 (2001).
19. A. N. Boto, P. Kok, D. S. Abrams, S. L. Braunstein, C. P. Williams, and J. P. Dowling, “Quantum interferometric optical lithography: exploiting entanglement to beat the diffraction limit,” *Phys. Rev. Lett.* **85**, 2733–2736 (2000).
20. I. Afek, O. Ambar, and Y. Silberberg, “High-NOON states by mixing quantum and classical light,” *Science* **328**, 879–881 (2010).
21. R. Morandotti, U. Peschel, J. S. Aitchison, H. S. Eisenberg, and Y. Silberberg, “Experimental observation of linear and nonlinear optical Bloch oscillations,” *Phys. Rev. Lett.* **83**, 4756–4759 (1999).
22. T. Pertsch, P. Dannberg, W. Elflein, A. Bräuer, and F. Lederer, “Optical Bloch oscillations in temperature tuned waveguide arrays,” *Phys. Rev. Lett.* **83**, 4752–4755 (1999).
23. H. Trompeter, W. Krolikowski, D. N. Neshev, A. S. Desyatnikov, A. A. Sukhorukov, Y. S. Kivshar, T. Pertsch, U. Peschel, and F. Lederer, “Bloch oscillations and Zener tunneling in two-dimensional photonic lattices,” *Phys. Rev. Lett.* **96**, 053903 (2006).
24. N. Malkova, I. Hromada, X. Wang, G. Bryant, and Z. Chen, “Observation of optical Shockley-like surface states in photonic superlattices,” *Opt. Lett.* **34**, 1633–1635 (2009).

25. Y. Plotnik, O. Peleg, F. Dreisow, M. Heinrich, S. Nolte, A. Szameit, and M. Segev, "Experimental observation of optical bound states in the continuum," *Phys. Rev. Lett.* **107**, 183901 (2011).
26. T. Schwartz, G. Bartal, S. Fishman, and M. Segev, "Transport and Anderson localization in disordered two-dimensional photonic lattices," *Nature* **446**, 52–55 (2007).
27. Y. Lahini, A. Avidan, F. Pozzi, M. Sorel, R. Morandotti, D. N. Christodoulides, and Y. Silberberg, "Anderson localization and nonlinearity in one-dimensional disordered photonic lattices," *Phys. Rev. Lett.* **100**, 013906 (2008).
28. L. Levi, M. Rechtsman, B. Freedman, T. Schwartz, O. Manela, and M. Segev, "Disorder-enhanced transport in photonic quasicrystals," *Science* **332**, 1541–1544 (2011).
29. B. Freedman, G. Bartal, M. Segev, R. Lifshitz, D. N. Christodoulides, and J. W. Fleischer, "Wave and defect dynamics in nonlinear photonic quasicrystals," *Nature* **440**, 1166–1169 (2006).
30. O. Peleg, G. Bartal, B. Freedman, O. Manela, M. Segev, and D. N. Christodoulides, "Conical diffraction and gap solitons in honeycomb photonic lattices," *Phys. Rev. Lett.* **98**, 103901 (2007).
31. T. Kitagawa, E. Berg, M. Rudner, and E. Demler, "Topological characterization of periodically driven quantum systems," *Phys. Rev. B* **82**, 235114 (2010).
32. F. D. M. Haldane, "Model for a quantum hall effect without Landau levels: condensed-matter realization of the "parity anomaly"," *Phys. Rev. Lett.* **61**, 2015–2018 (1988).
33. M. C. Rechtsman, Y. Lumer, Y. Plotnik, A. Perez-Leija, A. Szameit, and M. Segev, "Topological protection of path entanglement in photonic quantum walks," in *CLEO, OSA Technical Digest* (2015), paper FW4A.4.
34. S. Mittal, V. V. Orre, and M. Hafezi, "Topologically robust transport of entangled photons in a 2D photonic system," arXiv:1605.04894 (2016).